Mechatronics 21 (2011) 1183–1189

Contents lists available at ScienceDirect

Mechatronics

journal homepage: www.elsevier.com/locate/mechatronics

A miniature generator using piezoelectric bender with elastic base

W. Li [a], T.S. Liu [a,*], C.C. Hsiao [b]

[a] Department of Mechanical Engineering, National Chiao Tung University, Hsinchu 30010, Taiwan
[b] Mechanical and Systems Research Laboratories, Industrial Technology Research Institute, Hsinchu 31040, Taiwan

ARTICLE INFO

Article history:
Received 21 April 2010
Accepted 14 July 2011
Available online 10 August 2011

Keywords:
Miniature generator
Piezoelectric bender
Energy harvesting
Elastic base

ABSTRACT

Nowadays green energy devices such as vibration generators attempt to harvest energy from environment. A lot of studies dealing with vibration generators put emphasis on mechanism designs or power generation methods, but few on lowering the resonant frequency of power generation systems. This study proposes that elastic bases attached to vibration generators can lower natural frequencies, so as to make natural frequencies closer to ambient vibration frequency. Therefore, this study investigates miniature electric generators consisting of piezoelectric benders and elastic bases. To install the elastic base, this work uses a spring with prescribed stiffness and a board with given mass between the piezoelectric bender and a vibration source to make the resonant frequency of piezoelectric benders close to the frequency of ambient vibration. Analytical derivation is carried out to obtain optimal mass and stiffness. Accordingly, more electric power can be generated from piezoelectric generators using an elastic base with appropriate mass and stiffness. According to experimental results, using an elastic base increases 376 times generated power compared with no elastic base. In the presence of the elastic base, the power increases 132% when a point mass is added.

1. Introduction

For the sake of ubiquitous computing, micro-sensors are proposed to be embedded in isolated environment like human body or concrete walls. However, how to provide electric power into these sensors remains to be solved. One of solutions is green power harvesting. In recent years, without pollution and short-life problems of traditional batteries, several kinds of energy-harvesting designs have been proposed for green energy sources. These designs include acoustic energy collection, thermal energy collection, electromagnetic and electrostatic power transducers, vibration of piezoelectric materials, etc.

Williams and Yates [1] pointed out that mechanical energy can be used to generate electric power by a mass-spring-damper system. Vibration energy can be transformed into electric power by using transduction mechanisms such as piezoelectric, electromagnetic, and electrostatic devices. And if the mechanical system oscillates at a resonant frequency, the maximum power occurs. Therefore, in this study for performance of the miniature generator, it is beneficial to design a device with resonant frequency as close as possible to frequencies that human activities result in. However, resonant frequencies of miniature electromagnetic or electrostatic generators are too high to utilize. Hence, we focus on the piezoelectric generator in this paper. The electric power is generated by the strain change of piezoelectric benders. The strain change is caused by deformation of the piezoelectric bender in vibration. Starner [2] presented that computers can be powered by human motion such as swinging arms. Shenck and Paradiso [3] proposed that when the piezoelectric material embedded in human shoes is compressed, electric power is generated. Roundy et al. [4] powered a wireless sensor by using a low-frequency vibration source. Roundy et al. [5] pointed out that a trapezoidal-shaped piezoelectric bender can generate the maximum energy in the same volume. Xu et al. [6] presented that magnitudes of generated power are quite different by different loading methods. Kang et al. [7] presented that the power magnitude is proportional to the length while inversely proportional to thickness of the piezoelectric bender. The length is more effective than thickness. In the above studies, however, the vibration mechanisms in the above studies are all fixed to a rigid base, and the natural frequency of the vibration mechanism is relatively higher than the frequency of vibrations caused by natural environment or human-being. Marinkovic and Koser [8] proposed a harvesting platform using nonlinear stretch of fixed-fixed beams for a range of frequencies from 160 to 400 Hz, and aiming at 60 Hz. Cornwell et al. [9] proposed an auxiliary mechanism to make the resonant frequency closer to the frequency of the ambient vibration. Lipscomb et al. [10] presented that the resistance of piezoelectric ceramic varies with humidity and temperature. Sherrit et al. [11] presented that piezoelectric coefficients increase as temperature rises. Sharos et al. [12] proposed that eccentric attached masses and asymmetric

* Corresponding author.
E-mail address: tsliu@mail.nctu.edu.tw (T.S. Liu).

0957-4158/$ - see front matter © 2011 Elsevier Ltd. All rights reserved.
doi:10.1016/j.mechatronics.2011.07.004

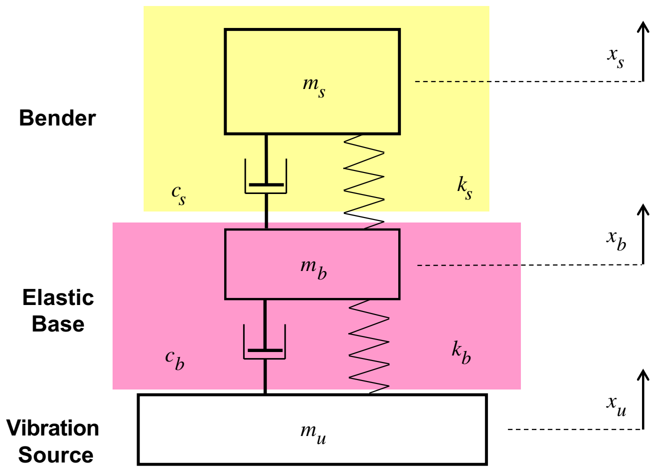

Fig. 1. Mass-spring model of piezoelectric bender attached to elastic base subject to excitation from vibration source.

cantilever geometry lead to modal coupling among bending, torsion, and lateral vibration. To reduce natural frequencies of miniature generators with piezoelectric benders, this paper proposes to use elastic bases, on which benders are installed, instead of a rigid base or auxiliary mechanisms.

2. Analytical model

In general, miniature generators are fixed to the ground or a vibration source rigidly. This paper compares vibration frequencies and generator powers between benders on a rigid base and benders on an elastic base. To study the miniature generator with a piezoelectric bender fixed to an elastic base, its dynamic model as shown in Fig. 1, will be analyzed first.

2.1. Elastic base

A miniature generator with a piezoelectric bender attached to a vibrating source elastically can be treated as two mass-spring systems in series. One is an equivalent system for the piezoelectric bender; the other is an equivalent system that accounts for the elastic-base effect, as shown in Fig. 1. In the equivalent system representing the piezoelectric bender, the equivalent mass, damping coefficient, and spring constant are denoted as m_s, c_s, and k_s, respectively. In the other equivalent system representing the elastic base, the equivalent mass, damping coefficient, and spring constant are denoted as m_b, c_b, and k_b, respectively. In addition m_u denotes the vibration source. If the vibration source is vibrating in a harmonic manner, its displacement x_u can be expressed by

$$x_u = A_u \sin\omega t \tag{1}$$

where A_u is the amplitude of the harmonic vibration at frequency ω. According to Fig. 1, the equation of motion for m_s can be written as

$$m_s\frac{d^2x_s}{dt^2} + c_s\frac{dx_s}{dt} - c_b\frac{dx_b}{dt} + k_s(x_s - x_b) = 0 \tag{2}$$

and the equation of motion for m_b can be written as

$$m_b\frac{d^2x_b}{dt^2} + (c_s + c_b)\frac{dx_b}{dt} - c_b\frac{dx_u}{dt} - c_s\frac{dx_s}{dt} + k_s(x_b - x_s) + k_b(x_b - x_u) = 0 \tag{3}$$

where x_b is the displacement of m_b, x_s is the displacement of m_s, k_s is the spring constant of the piezoelectric bender, k_b is the spring constant of the elastic base, c_s is the damping coefficient of the piezoelectric bender, and c_b is the damping coefficient of the elastic base.

When vibration resonance occurs, both displacements of m_s and m_b approach the maximum at the same frequency. They can be expressed as

$$x_s = A_s \sin\omega t \tag{4}$$

and

$$x_b = A_b \sin\omega t \tag{5}$$

where A_s is the vibration amplitude of the piezoelectric bender and A_b that of the elastic base. Substituting Eqs. (4) and (5) into Eqs. (2) and (3) gives

$$A_s(-m_s\omega^2\sin\omega t + c_s\omega\cos\omega t + k_s\sin\omega t) - A_b(c_b\omega\cos\omega t + k_s\sin\omega t) = 0 \tag{6}$$

and

$$A_s(-c_s\omega\cos\omega t - k_s\sin\omega t) - A_b[m_b\omega^2\sin\omega t + (c_s + c_b)\omega\cos\omega t - (k_s + k_b)\sin\omega t] = A_u(c_b\omega\cos\omega t + k_b\sin\omega t) \tag{7}$$

Eqs. (6) and (7) can be written as, in matrix form,

$$\begin{pmatrix} k_s\sin\omega t + c_s\omega\cos\omega t - m_s\omega^2\sin\omega t & -c_b\omega\cos\omega t - k_s\sin\omega t \\ -c_b\omega\cos\omega t - k_s\sin\omega t & (k_s + k_b)\sin\omega t - m_b\omega^2\sin\omega t - (c_s + c_b)\omega\cos\omega t \end{pmatrix}\begin{pmatrix} A_s \\ A_b \end{pmatrix} = \begin{pmatrix} 0 \\ A_u(c_b\omega\cos\omega t + k_b\sin\omega t) \end{pmatrix} \tag{8}$$

The resonance condition requires

$$\begin{vmatrix} k_s\sin\omega t + c_s\omega\cos\omega t - m_s\omega^2\sin\omega t & -c_b\omega\cos\omega t - k_s\sin\omega t \\ -c_b\omega\cos\omega t - k_s\sin\omega t & (k_s + k_b)\sin\omega t - m_b\omega^2\sin\omega t - (c_s + c_b)\omega\cos\omega t \end{vmatrix} = 0 \tag{9}$$

It can be written as

$$(k_s\sin\omega t + c_s\omega\cos\omega t - m_s\omega^2\sin\omega t) \times ((k_s + k_b)\sin\omega t - m_b\omega^2\sin\omega t - (c_s + c_b)\omega\cos\omega t) - (-c_b\omega\cos\omega t - k_s\sin\omega t) \times (-c_b\omega\cos\omega t - k_s\sin\omega t) = 0 \tag{10}$$

and be simplified to become

$$\left(\frac{\omega^4}{\omega_0^4}\right) + 2\xi\frac{(1 - a + d)}{a}\cot\omega t\left(\frac{\omega^3}{\omega_0^3}\right) - \left[\left(\frac{1 + r + a}{a}\right) + 4\xi^2\left(\frac{d^2 + d + 1}{a}\right)\cot^2\omega t\right]\left(\frac{\omega^2}{\omega_0^2}\right) + 2\xi\left(\frac{r - 3d}{a}\right)\cot\omega t\left(\frac{\omega}{\omega_0}\right) + \frac{r}{a} = 0 \tag{11}$$

where the mass ratio $a=\frac{m_b}{m_s}$, stiffness ratio $r=\frac{k_b}{k_s}$, damper ratio $d=\frac{c_b}{c_s}$, bender damping ratio $\xi=\frac{c_s}{2\sqrt{k_s m_s}}$, and bender natural frequency $\omega_0=\sqrt{\frac{k_s}{m_s}}$ are defined.

In general, four damping effects have to be considered: no damping, critical damping, underdamping, and overdamping. First, if the damping effect is neglected and thus $\xi = 0$, the bender damping ratio will be zero and Eq. (11) becomes

$$\left(\frac{\omega^2}{\omega_0^2}\right)^2-\left(1+\frac{1}{a}+\frac{r}{a}\right)\frac{\omega^2}{\omega_0^2}+\frac{r}{a}=0 \tag{12}$$

Solving Eq. (12) yields two solutions

$$\frac{\omega^2}{\omega_0^2}=\frac{\left[1+\frac{1}{a}(1+r)\right]\pm\sqrt{\left[1+\frac{1}{a}(1+r)\right]^2-\frac{4r}{a}}}{2} \tag{13}$$

However, the lower resonant frequency is concerned. Therefore, only the smaller solution is employed:

$$\frac{\omega^2}{\omega_0^2}=\frac{\left[1+\frac{1}{a}(1+r)\right]-\sqrt{\left[1+\frac{1}{a}(1+r)\right]^2-\frac{4r}{a}}}{2} \tag{14}$$

If the connection between m_b and m_u is rigid, k_b and hence r will approach infinity. Accordingly, Eq. (14) becomes

$$\frac{\omega^2}{\omega_0^2}=\frac{\left(1+\frac{r}{a}\right)-\sqrt{\left(1+\frac{r}{a}\right)^2-\frac{4r}{a}}}{2}=\frac{\left(1+\frac{r}{a}\right)-\sqrt{\left(1-\frac{r}{a}\right)^2}}{2}$$

Since $a \ll r$, and $1-\frac{r}{a}<0$,

$$\frac{\omega^2}{\omega_0^2}=\frac{\left(1+\frac{r}{a}\right)-\left[-\left(1-\frac{r}{a}\right)\right]}{2}=1$$

As a result,

$$\omega=\omega_0=\sqrt{\frac{k_s}{m_s}} \tag{15}$$

which is the same as the resonant frequency when the base is rigid and connected perfectly.

If the piezoelectric bender is overdamping, ξ will be greater than 1 in Eq. (11). If the piezoelectric bender is underdamping, $0 < \xi < 1$ in Eq. (11). If the piezoelectric bender is critical damping, $\xi = 1$. Eq. (11) thus becomes

$$\left(\frac{\omega^4}{\omega_0^4}\right)+2\frac{(1-a+d)}{a}\cot\omega t\left(\frac{\omega^3}{\omega_0^3}\right)-\left[\left(\frac{1+r+a}{a}\right)+4\left(\frac{d^2+d+1}{a}\right)\cot^2\omega t\right]\left(\frac{\omega^2}{\omega_0^2}\right)+2\left(\frac{r-3d}{a}\right)\cot\omega t\left(\frac{\omega}{\omega_0}\right)+\frac{r}{a}=0 \tag{16}$$

In fact, the piezoelectric bender damping ratio is usually very small, since its mechanical quality factor Q_m is 80 [13], from which $\xi=\frac{1}{2Q_m}=6.25\times10^{-3}$. Therefore, ξ can be treated as zero and Eq. (11) reduces to Eq. (12).

2.2. Stiffness of piezoelectric bender

A piezoelectric bender can be modeled as a spring as shown in Fig. 1, whose equivalent spring constant k_s in static condition can be written as [14]

$$k_s=k=\frac{3EI}{L^3} \tag{17}$$

where I is the area moment of inertia of the bender, E is the Young's modulus bender, L is the length, and m_s is the bender mass. However, in free vibration environment, resonant frequencies of the cantilever bender can be expressed by [14]

$$\omega_n=(\beta_n L)^2\sqrt{\frac{EI}{m_s L^3}},\quad n=1,2,3,\ldots \tag{18}$$

where $\beta_n L$ = 1.875, 4.694, 7.855, ... Compared to the definition $\omega_0=\sqrt{\frac{k_s}{m_s}}$, equivalent spring constants for all resonant frequencies can be expressed by

$$k=\frac{(\beta_n L)^2 EI}{L^3} \tag{19}$$

In this paper, the bender is made of ceramic piezoelectric material and is treated as a cantilever beam in modeling. The cantilever beam is further expressed by a linear spring with an equivalent spring constant, which however has been modified to account for vibration effects, as shown in Eq. (19). Because the bender material is ceramic of high stiffness and the vibration amplitude is small, large deformation of the bender does not happen. Hence, there is no nonlinear effect. Moreover, piezoelectric materials are temperature dependent [10,11]. For example, piezoelectric coefficients increase as temperature rises.

Since the first vibration mode is the main concern in this study, the equivalent spring constant in the first mode is $k=\frac{3.516EI}{L^3}$ instead of Eq. (17). In this study, $m_s = 3.969\times10^{-4}$ kg, $E = 5.8\times10^{10}$ Pa, and the dimension of the bender is 49 × 2.1 × 0.6 mm with piezoelectric length of 42 mm. The area moment of inertia is

$$I=\frac{bh^3}{12}=\frac{(2.1\times10^{-3})(0.6\times10^{-3})^3}{12}=3.78\times10^{-14}\ \mathrm{m}^4 \tag{20}$$

Thus, bender stiffness k_s can be calculated by using Eq. (19) as

$$k_s=\frac{(1.875)^2EI}{L^3}=\frac{3.516(5.8\times10^{10})(3.78\times10^{-14})}{(4.2\times10^{-2})^3}=104.04\mathrm{N/m} \tag{21}$$

Accordingly, the resonant frequency of the piezoelectric bender is calculated as

$$f_0=\frac{\omega_0}{2\pi}=\frac{\sqrt{\frac{k_s}{m_s}}}{2\pi}=\frac{\sqrt{\frac{104.04}{3.969\times10^{-4}}}}{2\pi}=81.2\ \mathrm{Hz} \tag{22}$$

2.3. Performance comparison

To investigate the elastic-base effect on lowering the resonant frequency, with definitions of mass ratio $a=\frac{m_b}{m_s}$ and stiffness ratio $r=\frac{k_b}{k_s}$, damper ratio $d=\frac{c_b}{c_s}$, and bender damping ratio $\xi=\frac{c_s}{2\sqrt{k_s m_s}}$, Eq. (11) can be used to compare the performances among different values of a, r, d, and ξ.

Since this study ignores the damping effect based on Section 2.1, Eq. (11) reduces to Eq. (12), where mass ratio a and stiffness ratio r are treated as design parameters for miniature generators.

Table 1
Normalized resonant frequencies ω/ω_0 when using various stiffness ratios $r=\frac{k_b}{k_s}$ and mass ratios $a=\frac{m_b}{m_s}$.

r \ a	1	4	8	10
1	0.62	0.44	0.33	0.30
2	0.77	0.60	0.47	0.42
4	0.88	0.78	0.64	0.59
6	0.92	0.87	0.76	0.71
8	0.94	0.91	0.84	0.80
10	0.95	0.93	0.89	0.86

Therefore, this study investigates how different a and r affect the resonant frequency. Given $a = 1, 4, 8, 10$ and $r = 1, 2, 4, 6, 8, 10$, calculating Eq. (14) results in normalized resonant frequencies as depicted in Table 1. According to Eq. (22), the theoretical resonant frequency ω_0 of the piezoelectric bender fixed to a rigid base equals to 81.2 Hz, which is closest to that with a rigid base shown in Fig. 5. Above all, according to Table 1, the use of elastic bases can lower the resonant frequency of miniature generators. With the same mass ratio a, as the stiffness ratio r increases, the resonant frequency of miniature generators increases and approaches that on the rigid base. However, under the same stiffness ratio r, as the mass ratio a increases, the resonant frequency of miniature generators decreases.

3. Experiment

3.1. Measurement of resonant frequency

This study also measures the resonant frequency of miniature generators on elastic bases. Springs with known spring constants are used in experiments so as to observe the effect of elastic bases of different stiffnesses on natural frequencies.

The experimental setup is illustrated in Fig. 2. An arbitrary waveform generator (AWG) generates a voltage signal to make a piezoelectric bender vibrate. A laser beam from a laser Doppler vibrometer (LDV) projects on the free end on the piezoelectric bender, and is detected also by LDV to become the displacement signal at the free end of the bender. The displacement signal is acquired by a dynamic signal analyzer and transformed into the frequency domain. The dynamic response and the resonant frequencies are thus obtained. Figs. 3 and 4 show photos of benders without and with an elastic base, respectively.

The measured spectrum of the piezoelectric bender on a rigid base is shown in Fig. 5, whose resultant resonant frequency is 85 Hz, close to the theoretical value of 81.2 Hz calculated in Eq. (22). The next step is to obtain the spectrum when using $a = 1, 4, 8, 10$ and $r = 1, 2, 4, 6, 8, 10$, respectively. The normalized frequency ω/ω_0 versus r is plotted with $\omega_0 = 85$ Hz. For comparison, Fig. 5 shows two measured spectrums of the bender installed on different elastic bases $a = 4$, $r = 10$, $a = 10$ and $r = 4$. The frequencies of largest peaks are lower than that of the rigid base. Figs. 6–9 depict frequency variation results of $a = 1, 4, 8$, and 10, respectively. For comparison, the theoretical normalized frequency ω/ω_0 from

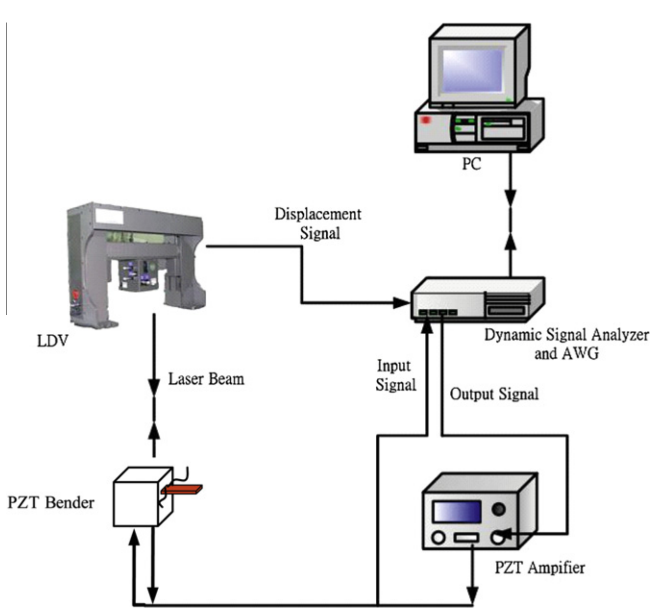

Fig. 2. Signal flow in experimental setup of piezoelectric bender.

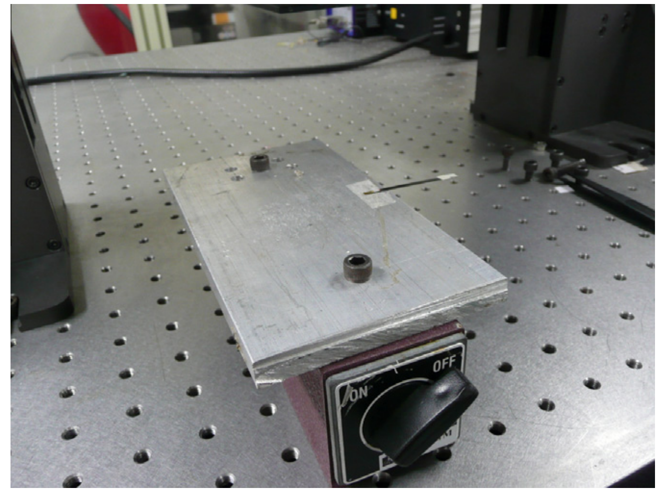

Fig. 3. Piezoelectric bender without elastic base.

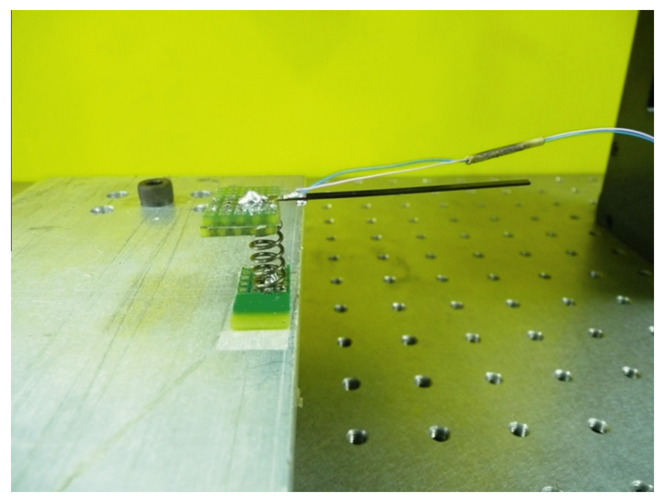

Fig. 4. Piezoelectric bender with elastic base.

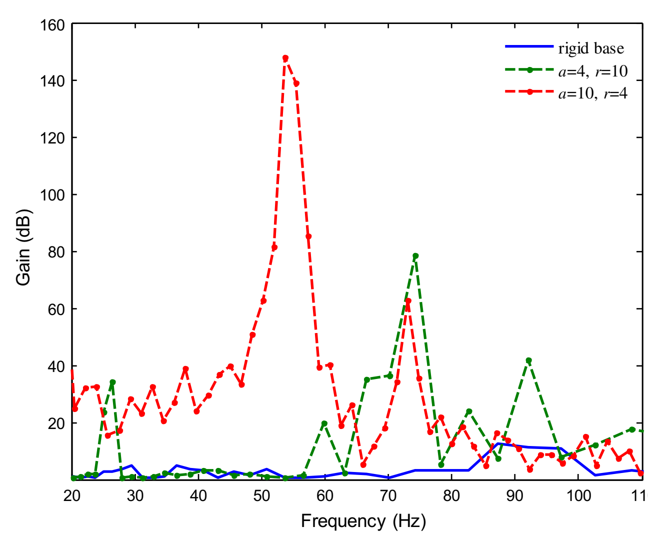

Fig. 5. Measured spectrums of piezoelectric bender on different bases.

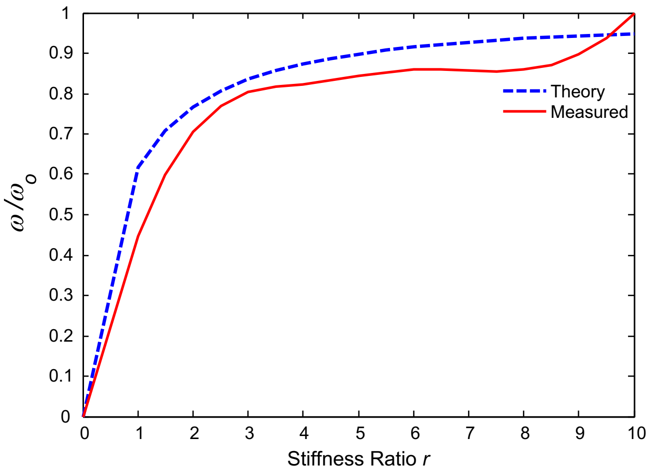

Fig. 6. Comparison between measured and theoretical results when mass ratio $a = 1$.

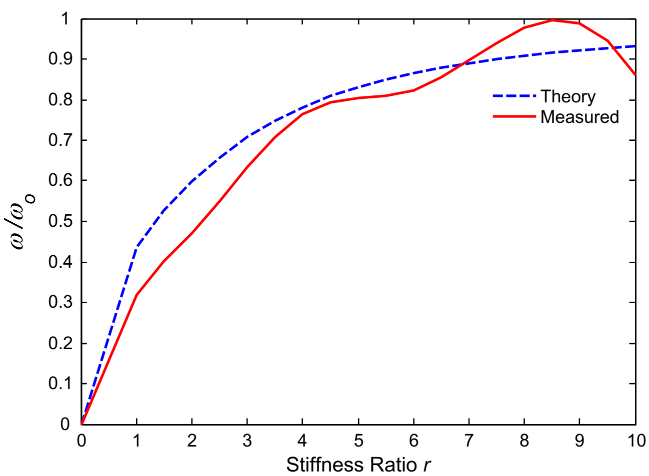

Fig. 7. Comparison between measured and theoretical results when mass ratio $a = 4$.

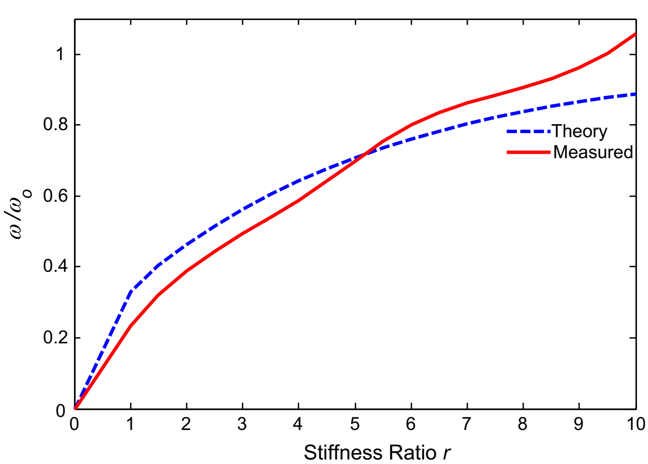

Fig. 8. Comparison between measured and theoretical results when mass ratio $a = 8$.

Eq. (14) is also plotted in the same figures. As a consequence, variations of resonant frequencies between measured and theoretical results are about the same.

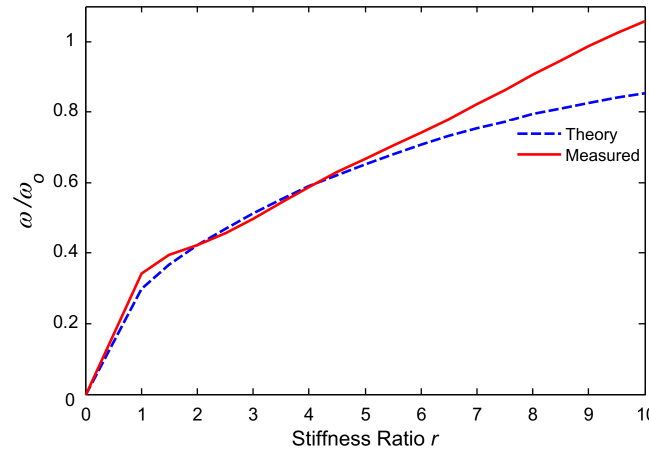

Fig. 9. Comparison between measured and theoretical results when mass ratio $a = 10$.

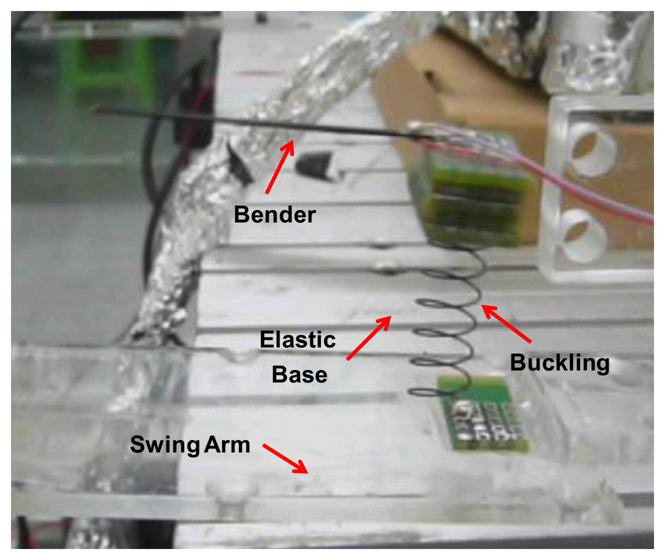

Fig. 10. Piezoelectric generator with elastic base and spring in buckling.

3.2. Shaking of the miniature generator

The photo of the present miniature generator is shown in Fig. 10. The piezoelectric bender is fixed to pieces of boards. And the boards are attached to a spring with known spring constant. The boards and the spring comprise the elastic base. The spring is fixed to a piece of board that is attached to a swing arm. Back-and-forth swing of the arm is driven by an electric motor. Vibration and hence deformation of the bender generate voltage and current, which are measured and recorded by a digital multimeter. For comparison, the same piezoelectric generator but with a rigid base is also measured and recorded in the same manner.

3.3. Power generation

Subject to vibration excitation arising from the electric motor, the arm swings within ±0.9° and the swing frequency is about 15 Hz. First, the miniature generator with a rigid base is attached to the swing arm for power generation. The maximum voltage and current measured are 12 mV and 0.09 μA, respectively. Hence, the corresponding maximum power is 1.08 nW. Second, the generator with an elastic base is attached to the swing arm.

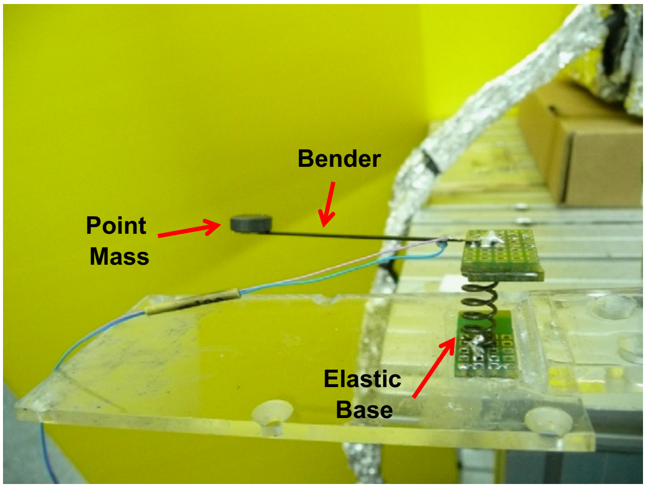

Fig. 11. Piezoelectric bender with elastic base and point mass.

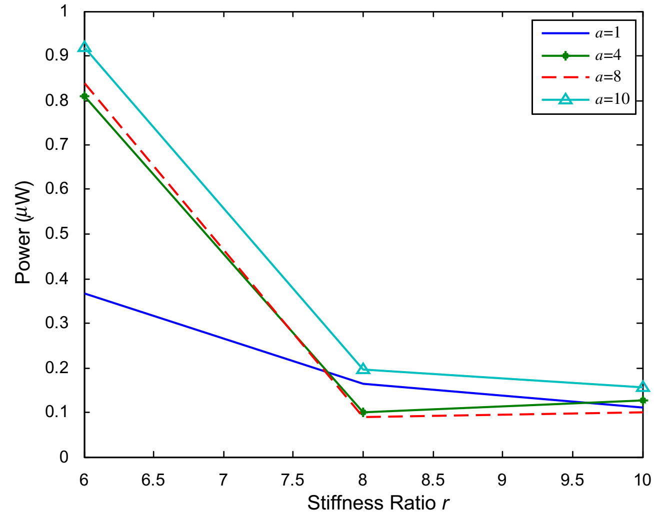

Fig. 12. Measured power generation from piezoelectric bender with elastic base.

Table 2
Measured voltage (mV) of bender in experiment when using various stiffness ratios $r = \frac{k_b}{k_s}$ and mass ratios $a = \frac{m_b}{m_s}$.

a / r	1	4	8	10
6	230	300	300	400
8	110	100	100	150
10	100	105	90	120

Table 3
Measured current (μA) of bender in experiment when using various stiffness ratios $r = \frac{k_b}{k_s}$ and mass ratios $a = \frac{m_b}{m_s}$.

a / r	1	4	8	10
6	1.6	2.7	2.8	3.2
8	1.5	1.0	0.9	1.3
10	1.1	1.2	1.1	1.3

Table 4
Measured power (μW) of bender in experiment when using various stiffness ratios $r = \frac{k_b}{k_s}$ and mass ratios $a = \frac{m_b}{m_s}$.

a / r	1	4	8	10
6	0.368	0.81	0.84	0.92
8	0.165	0.10	0.09	0.195
10	0.11	0.126	0.099	0.156

By changing elastic bases, different maximum voltages and currents are recorded. Long springs with small spring constants may not be strong enough to maintain compression and elongation in the longitudinal direction of the spring, such that transverse movement of the spring may happen and buckling occurs.

In the case without any point mass attached to the end of piezoelectric bender, when stiffness ratio $r = 1$, spring buckling occurs, as shown in Fig. 10. When $r = 4$ and $a = 2$ the maximum power generated in the case without any point mass is 396 nW, which is 376 times of a rigid base in use.

A point mass is in turn attached to the free end of the piezoelectric bender to generate electric power as shown in Fig. 11, and the point mass is 0.9 g. However, buckling is easier to occur when using a point mass. In this case with a point mass, the buckling not only happens at $r = 1$, but also happens at $r = 2$, 4. Therefore, only the power generation of $r = 6$, 8, 10 are recorded. By changing elastic bases, different voltages and currents are recorded and listed in Tables 2 and 3, respectively. The corresponding powers are listed in Table 4 and Fig. 12. The maximum power generated in the case with a point mass is 0.92 μW when $r = 6$ and $a = 10$, which is 2.4 times of that using an elastic base without any point mass. Based on Table 4, under the same mass ratio, the generator power decreases as the stiffness ratio increases. When the stiffness ratio is close to 10, the resonant frequency is also close to that of the miniature generator on the rigid base. For the resonant frequency far away from the vibration source frequency, the generator power decreases when the stiffness ratio r is not smaller than 10. The same trend is observed with fixed stiffness ratio while increasing the mass ratio.

According to the theory of eigenvalue veering [12], previously uncoupled vibration modes are expected to couple strongly in the presence of eccentric attached masses and asymmetric cantilever geometry. Therefore, in the presence of eccentric mass or asymmetric geometry, the piezoelectric bender would show modal coupling among bending, torsion, and lateral vibration.

4. Conclusions

For the purpose of increasing generated power in harvesting energy, according to Eq. (14) that has been derived in this paper, the elastic base can indeed lower the resonant frequency of the miniature generator to approach ambient vibration frequency. The resonant frequency reduction percentage depends on mass and stiffness of the proposed elastic base. Based on Eq. (14) and Table 1, the resonant frequency reduction percentage can reach 70% when $r = 1$ and $a = 10$. If the miniature generator is attached to the rigid base, the maximum power is 1.08 nW. By contrast, if the miniature generator is attached to an elastic base with a point mass, the maximum value of the power 0.92 μW is obtained with the mass ratio $a = 10$ and stiffness ratio $r = 6$. The power of different cases on elastic base with point mass is shown in Table 4.

In this study, the arm swing frequency is designated as 15 Hz, and the theoretical resonant frequency of the miniature generator of piezoelectric bender shown in Eq. (22) is about 81.2 Hz. According to Table 1, when the stiffness ratio r is fixed if the mass ratio a increases, the resonant frequency decreases and is close to 15 Hz, the arm swing frequency. Therefore, the bender vibration amplitude becomes larger. The more the bender deforms, the more power is generated. For example, Table 4 shows that when $r = 6$, more power is generated as the mass ratio a increases. However, if the mass ratio a is fixed but stiffness ratio r increases, the resonant frequency increases and is far away from 15 Hz. Consequently, the vibration amplitude decreases. Smaller deformation generates less power. Table 4 shows that when $a = 10$, less power is generated as the stiffness ratio r increases.

When appropriate stiffness ratio and mass ratio are chosen, the presence of an elastic base can indeed reduce the resonant frequency of the generator and approach the frequency that human can produce. As a consequence, experimental results show that the presence of elastic bases than the absence increases 376 times output power. Therefore, the appendage of elastic bases is beneficial to miniature generators in harvesting the vibration energy from human activities.

Concerning the vision of the proposed miniature generator, its real application lies in portable electronic devices and ubiquitous computing. To reduce charging times of portable electronic devices such as cell phones, the proposed generator utilizes ambient vibration energy to generate electric energy. In addition, to realize ubiquitous computing requires numerous sensors, which demand electric energy coming from ambient environment like what the present study proposes. Nevertheless, it remains to shrink the volume of the proposed miniature generators before they can be put into practical use, for which the microelectromechanical system (MEMS) technology may have to be applied.

Acknowledgements

This work was supported by National Science Council in Taiwan under Grant Number NSC96-2221-E009-146.

References

[1] Williams CB, Yates RB. Analysis of a micro-electric generator for microsystems. Sensors Actuators 1996;52:8–11.
[2] Starner T. Human-powered wearable computing. IBM Syst J 1996;35:1898–902.
[3] Shenck NS, Paradiso JA. Energy scavenging with shoe-mounted piezoelectrics. IEEE Micro 2001;21:30–42.
[4] Roundy S, Wright PK, Rabaey J. A study of low level vibrations as a power source for wireless sensor nodes. Comput Commun 2003;26(11):1131–44.
[5] Roundy S, Leland ES, Baker J, Carleton E, Reilly E, Lai E, et al. Riverside improving power output for vibration-based energy scavengers. IEEE Pervas Comput 2005;4(1):28.
[6] Xu CN, Akiyama M, Nonaka K, Watanabe T. Electrical power generation characteristics of PZT piezoelectricceramics. IEEE Trans Ultrason Ferroelect Freq Control 1998;45(4):1065–70.
[7] Kang JY, Kim HJ, Kim JS, Kim TS. Optimal design of piezoelectric cantilever for a micro power generator with microbubble. In: Microtechnologies in medicine & biology 2nd annual international IEEE-EMB special topic conference; 2002. p. 424–7.
[8] Marinkovic B, Koser H. Smart sand – a wide bandwidth vibration energy harvesting platform. Appl Phys Lett 2009;94:103505.
[9] Cornwell P, Goethal J, Kowko J, Damianakis M. Enhancing power harvesting using a tuned auxiliary structure. J Intell Mater Syst Struct 2005;16(10):825–34.
[10] Lipscomb IP, Weaver PM, Swingler J, McBride JW. The effect of relative humidity, temperature and electrical field on leakage currents in piezo-ceramic actuators under dc bias. Sensors Actuat A Phys 2009;151:179–86.
[11] Sherrit S, Yang G, Wiederick HD, Mukherjee BK. Temperature dependence of the dielectric, elastic and piezoelectric material constants of lead zirconate titanate ceramics. In: Proceedings of international conference on smart materials structure and systems, vol. 7–10; 1999. p. 121–6.
[12] Sharos LB, Raman A, Crittenden S, Reifenberger R. Enhanced mass sensing using torsional and lateral resonances in microcantilevers. Appl Phys Lett 2004;84:4638–40.
[13] <http://www.americanpiezo.com/apc-materials/piezoelectric-properties.html>. APC International, Ltd.
[14] Rao SS. Mechanical vibrations. 2nd ed. Addison-Wesley Publishing Company; 1990.